

# **A simple all-inorganic hole-only device structure for monitoring the trap densities in perovskite solar cells**

**Atena mohamadnezhad<sup>1</sup>, Mahmoud Samadpour<sup>1\*</sup>**

<sup>1</sup>Department of Physics, K. N. Toosi University of Technology, Tehran, Iran  
samadpour@kntu.ac.ir

## **ABSTRACT**

One of the most critical challenges in soaring the performance of perovskite solar cells is decreasing the density of trap states in the light-absorbing perovskite layer. These traps cause an increase in the recombination of charge carriers and decrease the efficiency of devices. One of the methods to study the trap density is space charge limited current (SCLC) analysis. For this purpose, some structures are needed with the ability to transport only electrons or holes. The trap density can be calculated by investigating the current-voltage diagram and finding the voltage corresponding to the slope change point. One of the challenges in these structures is using organic polymers like Spiro-OMeTAD, PEDOT: PSS, and PTAA as hole transport layers. They have problems like high acidity, lack of stability against moisture, low charge mobility, low conductivity, and high cost. In this work, a hole-only device structure is explained, made based on inorganic materials, which possesses high stability, a simple preparation method, and reasonable cost compared to conventional hole-only device structures. This structure is built by coating a nanostructured NiOx layer, perovskite, CIS, and Au on the ITO substrate. To investigate the performance of this structure, various perovskite layers were made at different experimental conditions, and their trap density was obtained by the proposed hole-only device structure. The analysis of the photovoltaic characteristics of cells revealed a clear correlation between the perovskite layer's trap density and the cells' performance. Our results show the introduced structure is a simple and stable structure that can be utilized in studying the trap density in perovskite layers to make more efficient cells.

## 1. INTRODUCTION

Environmental issues and the non-renewability of fossil fuels are the main factors that make the human race focus on devices capable of converting renewable energy like solar to other energy types like electricity. In this regard, the new generation of photovoltaic cells like perovskite solar cells (PSCs) have attracted considerable attention in recent years, which is originated by the unique properties of the perovskite material.

Perovskite has an  $ABX_3$  general structure: A is a large cation like formamidinium or methylammonium, B is a smaller cation like Pb or Sn, and X is a halogen. Every halogen atom is surrounded by four cations in the A site and two in the B site so that a  $BX_6$  octahedral would be formed and an extensive A site cation would be placed in B-X octahedral holes. Perovskite can easily make from chemical solution precursors at low temperatures, while its optoelectronic properties can be adjusted by simple chemical substitution methods without considerable change in its general properties. Besides the high light absorption in the visible and IR range, perovskite has a high charge carrier mobility. Alongside the exciting properties, some challenges must be addressed for further efficiency improvement of perovskite cells for practical applications. These include the poor

stability of perovskite under ambient conditions, primarily moisture, low thermal stability, energy mismatch at the interface of the perovskite/ETL&HTL layers, crystalline defects, and bulk/surface trap states in the perovskite structure, etc.

For example, surface defects in perovskite layers cause a noticeable increase in charge recombination and decrease cell efficiency. These defects are divided into shallow and deep levels and create transition levels in the band gap. The shallow levels form near the valence or conduction band, creating unwanted doping, which may facilitate charge transfer. Deep levels are formed in forbidden regions, and trapped charge carriers can't quickly transfer to valence or conduction energy levels. Therefore, they form charge recombination centers and cause a decrease in the efficiency of perovskite solar cells [1].

Perovskite defects include atomic vacancy, interstitial defects, and substitutional defects. Cation vacancy causes shallow traps, but other defects like anion vacancy, substitutional defects, or interstitial defects cause deep traps [2]. While it is expected that the bonding in perovskite lattice to be ionic, some defects can cause powerful covalence bonding and are one of the reasons for deep traps in perovskite structures. Regarding the crucial role of trap states on the

performance of the perovskite layer, it is imperative to explore them quantitatively. Therefore, designing simple and effective methods to study the density of trap states is required. Various methods are explained before to achieve this, like the density functional theory (DFT) method, transient photo-voltage (TPV), and SCLC. The accuracy of the DFT method depends on the correct choice of the model, and this issue creates complications in the calculations [3, 4]. TPV method only works with the assumption of zero temperature and exponential density of states (DOS), and it is not easy to analyze its data [5].

SCLC analysis is one of the simplest and most effective ways to study the distribution of semiconductor traps. This method obtains the current density by applying a voltage to the under-study device. The contiguity of the charge injector layer must be an ohmic contact, so the charge can be injected without facing a potential barrier. On the other hand, the second contiguity must be selected in such a way as to prevent the injection of opposite charge carriers. SCLC analysis is conducted in two ways: transient dark injection and steady-state used for relatively thin layers [6].

Theoretically J-V diagram should show four regimes. The first is an ohmic regime in which the current transfer is primarily because of the

intrinsic charge carriers of the semiconductor. As it is clear from the name of this regime, the current follows Ohm's law in this region. With increasing the electrical potential and charge entry from electrodes into the semiconductor, the dominant charge carriers in the current flow are these injected charges. In this region, a uniform density of charge carriers is formed in the semiconductor. The current is limited due to the created space charge and follows Mott-gurney's law [7]. In this region, charge transfer time is less or equal to the dielectric relaxation time. The trapping of charges is started by increasing the charge carrier's energy and reaching existing trap energy levels in the semiconductor. This condition lets more charge carriers enter the semiconductor, and the slope of the graph increases significantly. This regime is named the trap filling regime. When all of the traps are filled fourth area begins. In this region, current follows Mott-gurney's law again. But these areas cannot be observed in the actual SCLC diagram because the traps of semiconductors are scattered at different levels. However, by finding the breaking point of the diagram ( $V_{TFL}$ ), trap density is easily obtained from the following formula [8].

$$V_{TFL} = \frac{1}{2} \frac{eN_{trap}L^2}{\epsilon_0\epsilon}$$

In this equation,  $V_{TFL}$  is trap-filled limit voltage,  $\epsilon_0$  is the electrical permittivity of vacuum,  $\epsilon$  is the relative permittivity of perovskite (28.8),  $L$  is the

thickness of the perovskite,  $e$  is the fundamental charge value, and  $N_{\text{trap}}$  is the trap density [8]. Until now, many researchers have used the mentioned method to calculate the density of traps in perovskite solar cells and to optimize their efficiency.

For example, R. Li et al., who succeeded in making a solar cell with an efficiency of about 21%, used the ITO/NiOx/perovskite/Spiro-OMeTAD/Au structure in SCLC analysis to calculate the trap density of perovskite and the obtained trap density was  $2.56 \times 10^{16} \text{cm}^{-3}$ [9]. Also, X.Zhu et al. were able to obtain 23.25% efficiency by reducing the surface trap density of perovskite using 1,3-dimethyl-3-imidazolium hexafluorophosphate (DMIMPF<sub>6</sub>) ionic liquid. In their study to calculate trap density, FTO/NiOx/perovskite/Spiro-OMeTAD/Au hole only device structure was used, and trap density obtained  $6.04 \times 10^{15} \text{cm}^{-3}$ [10]. J.Yuan et al. used CsPbI<sub>2</sub>Br perovskite to reduce deep defects, and they used SCLC analysis with FTO/TiO<sub>2</sub>/perovskite/PCBM/Ag structure to obtain the trap density. The trap density obtained in their research was  $6.64 \times 10^{16} \text{cm}^{-3}$  [11].

H. Xu et al. increased the stability and efficiency of solar cells by using a 2D perovskite layer on the main perovskite layer. For trap density calculation, they applied SCLC analysis with

FTO/TiO<sub>2</sub>/Perovskite/PCBM/Ag structure, and the trap density obtained  $4.75 \times 10^{15} \text{cm}^{-3}$  [12].

Y.Su et al. used ITO/SnO<sub>2</sub>/2D perovskite/PCBM/BCP/Ag in SCLC analysis to control 2D perovskite morphology and trap density obtained  $0.66 \times 10^{15} \text{cm}^{-3}$ [13]. ZH.Gao et al. utilized benzophenone to improve the morphology of monocrystalline perovskite film. Trap density with ITO/PCBM/Perovskite/PCBM/Ag structure and adding 5 wt% benzophenone was calculated at  $8.9 \times 10^{15} \text{cm}^{-3}$ [14]. X. Wu et al. doped perovskite film with Eu<sup>2+</sup> to increase the stability of perovskite film. Also, this doping showed a reduction in the trap density of the perovskite layer. They used SCLC analysis to study trap density with FTO/SnO<sub>2</sub>/Perovskite/PCBM/Ag structure and achieved  $2.67 \times 10^{15} \text{cm}^{-3}$  trap density [15].

S.Wang et al. used cetyl trimethyl ammonium bromide (CTABr) to passivate perovskite defects and improve moisture stability. In the sequel to study trap density, they used two structures for SCLC analysis: ITO/SnO<sub>2</sub>/perovskite/CTABr/PCBM/Au and ITO/PEDOT: PSS/Perovskite/CTABr/Spiro-OMeTAD/Au, electron-only and hole-only devices respectively and they obtained  $4.53 \times 10^{15}$  and  $3.60 \times 10^{15} \text{cm}^{-3}$  trap density respectively [16]. B. Cao et al. used single-

capacity cations K and Rb in perovskite to improve PCE and decrease recombination. Moreover, with SCLC analysis in FTO/SnO<sub>2</sub>/perovskite/PCBM/Au structure, they find out that trap density reduces from  $2.75 \times 10^{16}$  to  $1.33 \times 10^{16} \text{cm}^{-3}$  [17]. M. Han et al. studied the effect of cesium doping on lead(II)-acetate-based perovskite solar cells. Their study confirmed the growth in PCE from 14.1 % to 15.57 %. Besides, the ITO/PTAA/Perovskite/PTAA/Ag structure was used in SCLC analysis, and the trap density was  $3.6 \times 10^{16} \text{cm}^{-3}$  in the modified sample [18]. J. Zhang et al. achieved 20.7% efficiency through 1% Sr doping in NiO<sub>x</sub> by increasing electrical conductivity, perovskite crystallization, and adjusting the energy level of perovskite and nickel oxide. Trap density with FTO/Sr:NiO<sub>x</sub>/Perovskite/MoO<sub>x</sub>/AgAl structure obtained  $1.7 \times 10^{16} \text{cm}^{-3}$  [19].

D. Yao et al. enhanced the stability of a perovskite device by adding Tri ethylene tetramine (TETA) to control material dimensions, and they got  $1.02 \times 10^{16} \text{cm}^{-3}$  trap density using SCLC analysis by FTO/SnO<sub>2</sub>/Perovskite (treated with TETA)/PCBM/Ag structure [20]. M. Jiang et al. used P<sub>3</sub>HT to affect the grain boundaries and modify the perovskite defects. This method increases PCE and passivates the surface traps. In addition, it causes a superior energy level matching between the valence band of the

perovskite layer with the hole transport layer. FTO/PEDOT: PSS/Perovskite/Spiro-OMeTAD/Ag structure was used in SCLC analysis, and the trap density was  $1.12 \times 10^{16} \text{cm}^{-3}$  [21].

Wu et al. reduced the defect density using PEAI and increased the efficiency in FTO/SnO<sub>2</sub>/CsPbBr/PCBM/Au structure, while the trap density achieved  $0.66 \times 10^{16} \text{cm}^{-3}$  [22]. Lio et al. used Cu<sup>2+</sup> in their perovskite device to increase the crystallization and improve the morphology. Also, it decreased trap density and recombination, which led to enhanced PCE and stability. The SCLC analysis in the hole-only device FTO/PEDOT: PSS/Perovskite/Spiro-OMeTAD/Ag and electron-only device FTO/TiO<sub>2</sub>/perovskite/PCBM/Ag was conducted, and trap density obtained  $5.78 \times 10^{15}$  and  $2.60 \times 10^{15} \text{cm}^{-3}$  respectively [23].

S. Kim et al. used butyl acetate (BA) and chlorobenzene (CB) to improve perovskite film morphology. These two materials have similar physical properties, but BA is less toxic, improving the charge mobility and PCE. With SCLC analysis, these films were applied in ITO/PEDOT: PSS/Perovskite/Spiro-OMeTAD/Ag hole only and ITO/SnO<sub>2</sub>/Perovskite/PCBM/Ag electron only structures and trap density of BA-perovskite indicated to be  $2.42 \times 10^{15} \text{cm}^{-3}$  for hole-only

device and  $1.65 \times 10^{15}$  for electron-only device that shows an improvement comparing to CB-perovskite [24]. J. Yung et al. replaced the PCBM electron transport layer with CeO in the perovskite device structure so that perovskite has more resistance against moisture. According to the SCLC analysis with ITO/TiO<sub>2</sub>/perovskite/ETL/Ag structure, trap density decreased from  $3.98 \times 10^{16}$  to  $3.15 \times 10^{16} \text{ cm}^{-3}$  after PCBM replacement [25]. X. Zhang et al. achieved  $1.4 \times 10^{15} \text{ cm}^{-3}$  trap density with ITO/PEDOT: PSS/MAPI<sub>3</sub>/P<sub>3</sub>HT/Au structure. Although the obtained trap density was low, using the organic hole transport layer caused a reduction in device stability [26]. J. Yau et al. modified the perovskite with DAGCI (6%) in ITO/Poly TPD/Perovskite/PTAA/MoO<sub>x</sub>/Ag structure and reduced the trap density from  $3.4 \times 10^{16}$  to  $2.4 \times 10^{16} \text{ cm}^{-3}$  [27]. G. Tang et al. made ITO/PTAA/Perovskite/Au structure, and they modified perovskite with MoS<sub>2</sub>, and trap density reduced from  $1.17 \times 10^{16} \text{ cm}^{-3}$  in pristine cell to  $0.53 \times 10^{16} \text{ cm}^{-3}$  in the modified cell [28]. X. Liu et al. modified perovskite with t-BAI (0.01%) in glass/FTO/PEDOT: PSS/Perovskite/Au structure. SCLC analysis trap density of perovskite with and without t-BAI was obtained at  $8.77 \times 10^{16} \text{ cm}^{-3}$  and  $4.54 \times 10^{16} \text{ cm}^{-3}$  respectively [29]. W. Li et al. modified perovskite with organic ligands, TOPO

and TPPO. Their structure was FTO/PEDOT: PSS/Perovskite/SpiroOMeTAD/Au, and trap density obtained  $4.2 \times 10^{16}$ ,  $2.03 \times 10^{16}$  and  $1.78 \times 10^{16} \text{ cm}^{-3}$  for pristine, TOPO, and TPPO modified cells, respectively [30]. F. Pinar et al. made glass/ITO/NiO<sub>x</sub>/CH<sub>3</sub>NH<sub>3</sub>PbI<sub>3</sub>/P<sub>3</sub>HT/Au structure in which NiO<sub>x</sub> was doped with Li mixed with Co, Li mixed with Mg, and Co mixed with Mg. Trap density values reduced from  $11.08 \times 10^{15}$  to  $7.09 \times 10^{15} \text{ cm}^{-3}$  while using the organic polymer reduced the thermal stability [31].

As evident from the mentioned researches, organic charge transport materials are widely utilized in perovskite cells, and electron/hole-only devices by various researchers. Although organic charge transport materials show attractive efficiencies in photovoltaic devices, some challenges in using them push the researchers to focus on inorganic materials as a candidate for charge transport materials instead. For example, Spiro-OMeTAD is one of the most used materials in perovskite devices. This material has low hole mobility, and making a uniform thin film is difficult. Moreover, it has low stability against moisture [32]. The other usual hole transport material is PEDOT: PSS, whose hydrophilic nature makes it unstable against moisture.

Additionally, its acidity causes some reactions with perovskite over time that degrade the device [33]. PTAA is one of the commonly used hole transport materials which was used in photovoltaic devices. Because of its low mobility, it needs to be doped with other materials to have a proper function in photovoltaic devices. Still, doping has a negative effect on the device's hysteresis [34]. Besides the different HTL materials, various ETLs are also utilized in perovskite cells until now. SnO<sub>2</sub> is a conventional electron transport material, but pure SnO<sub>2</sub> has low mobility, high hysteresis, and large trap density [35]. NiO<sub>x</sub> is an inorganic material with high hole mobility [36] and low absorption in the absorption region of perovskite [37]. The stability of this material against moisture and environmental conditions would improve the stability of the device. Also, its valence energy level is close to perovskite valence energy, making it suitable for contact with perovskite.

One of the typical ETLs is TiO<sub>2</sub>, whose absorption intersects with the perovskite absorption region [38]. So, it absorbs some of the incident light and reduces the number of photons arriving at the perovskite layer. Besides, it increases the recombination rate when transporting electrons by producing electron and hole pairs by absorbing light [39]. MoO<sub>x</sub> can also use as an electron transport material, while its

parasitic absorption at wavelengths longer than 600 nm and its low thermal stability are the main challenges [40].

This study introduces a new structure based on all inorganic layers for SCLC analysis with ITO/NiO<sub>x</sub>/Perovskite/CIS/Au structure. In this hole-only device, ITO is the substrate, NiO<sub>x</sub> and Copper indium selenide (CIS) are inorganic hole transfer layers, the perovskite layer is between them, and finally, gold electrode (Au) is deposited on CIS. CIS is an inorganic HTL recently applied in perovskite solar cells successfully [41]. It has good conductivity and is a stable material with a proper valence energy level relative to the perovskite, making it a suitable choice for extracting holes from perovskite [42].

Using inorganic NiO<sub>x</sub> and CIS HTLs, stable hole-only devices were successfully made for SCLC measurements with stable and low-cost materials. Various PSCs were made to confirm the performance of our suggested hole-only device structure, and their performance was correlated to the density of trap states obtained by the suggested all-inorganic hole-only device structure. Our result reveals that the introduced structure is a simple and stable device that can be utilized in studying the trap densities in perovskite layers, to make more efficient cells.

## 2. Experimental Section

### 2.1 Materials and synthesizing methods

Fluorine-doped tin oxide (FTO) coated glass substrates were patterned with Zinc powder and diluted hydrochloric acid. Patterned samples were respectively sonicated by Hellmanex, deionized water, ethanol, acetone, and isopropanol solution within 10 minutes for each solution. FTO samples were then annealed at 450 °C for 15 min and placed under a UV-Ozone atmosphere to remove the remained contaminations. To deposit the TiO<sub>2</sub> hole-blocking layer on FTO, the 0.15 M TTIP solution in ethanol was spin coated at 2000 rpm for 30 secs and then annealed for an hour at 500 °C. Afterward, a commercial TiO<sub>2</sub> paste was diluted in ethanol (1 to 5.5 weight ratio), spin coated at 4000 rpm on the FTO/compact TiO<sub>2</sub> layer for 30 secs, and sintered at 500 °C for 30 min. Before the deposition of the perovskite layer, FTO/block-TiO<sub>2</sub>/meso-TiO<sub>2</sub> layers were put under UV-O<sub>3</sub> treatment for 5 min.

To prepare the perovskite precursor, PbI<sub>2</sub> (1.1 M), FAI (1 M), MABr (0.2 M), CsI (0.05 M), and PbBr<sub>2</sub> (0.22 M) were dissolved in anhydrous DMF: DMSO solvent (4:1 volume ratio). In two steps, the perovskite layer was spin coated on the prepared TiO<sub>2</sub> mesoporous layer. First, with 1000 rpm for 10 secs and then with 4000 rpm for 20 secs while the 250 microliters of

chlorobenzene anti-solvent is added at the last 5 secs of the second spin coating step.

Also, some modified perovskite layers were prepared by utilizing a different anti-solvent material which was prepared by adding TEOS into the chlorobenzene with volume ratios of 3 and 400, respectively. The as-prepared perovskite layers were annealed at 100°C for one hour to increase the crystallization. A thin Spiro-OMeTAD hole-transport layer was spin coated on the perovskite layer at 500 rpm for 30 s. The HTL precursor was obtained from a solution containing 72.3 mg Spiro-OMeTAD (99.5%, Borun Co, China) in 1 ml of chlorobenzene, 28.8 µl 4-tert-butylpyridin, and 17.5 µl of a 1.8 M LiTFSI solution in acetonitrile. Finally, gold contacts (~100 nm thickness) were thermally deposited to complete the devices. The hole-only devices had an ITO/NiOx/Perovskite/CIS/Au configuration, where ITO is the substrate and the hole collector electrode. NiOx and CIS are the hole-transporting layers and were prepared according to the methods we explained before [43, 41].

### 2.2. Characterization Methods

X-ray diffraction patterns were acquired by X'Pert Pro MPD equipment with Cu K $\alpha$  ( $\lambda=1.54$



Å) radiation. SEM micrographs were recorded using a MIRA3 TESCAN field emission scanning electron microscope. Optical properties of the perovskite layers were taken with a UVS-2500 spectrometer from PHYSTEC Company. The photocurrent-voltage measurements were performed under standard AM 1.5 ( $1000 \text{ W/m}^2$ ) simulated light radiation by a Sharif Solar SIM-1000 system (calibrated by a Thorlabs photodiode). A Keithley 2400 digital source

### 3. RESULTS AND DISCUSSION

SEM images of the pristine and TEOS-modified perovskite layers are provided in Figure 1. As apparent from this figure, a negligible difference could be explored in surface morphology, and large grain sizes are evident in both layers with or without modifications. The crystalline structure of the pristine and modified perovskite films is characterized by X-ray diffraction (XRD), as illustrated in Figure 2. The diffraction peaks at  $14.10$ ,  $20.03$ ,  $24.56$ ,  $28.43$ ,  $31.86$ ,  $40.64$ , and  $43.28^\circ$  corresponding to the crystalline planes of the photoactive black phase of  $\text{Cs}_{0.05}(\text{MA}_{0.17}\text{FA}_{0.83})_{0.95}\text{Pb}(\text{I}_{0.83}\text{Br}_{0.17})_3$  perovskite layer [13]. Meanwhile, there is no diffraction peak from the undesired photo inactive delta phase of  $\text{FAPbI}_3$  at  $11.61^\circ$ , a common and not preferred side structure in three cationic perovskite layers.

meter recorded the J- V curves while the cells were masked during the measurement with an active area of  $0.16 \text{ cm}^2$ . SCLC measurements were conducted on hole-only devices with ITO/NiOx/Perovskite/CIS/Au architecture. For the steady-state photoluminescence (PL) measurements, samples were excited by a 350 nm laser, and an Avaspec 2048 TEC spectrophotometer acquired emissions.

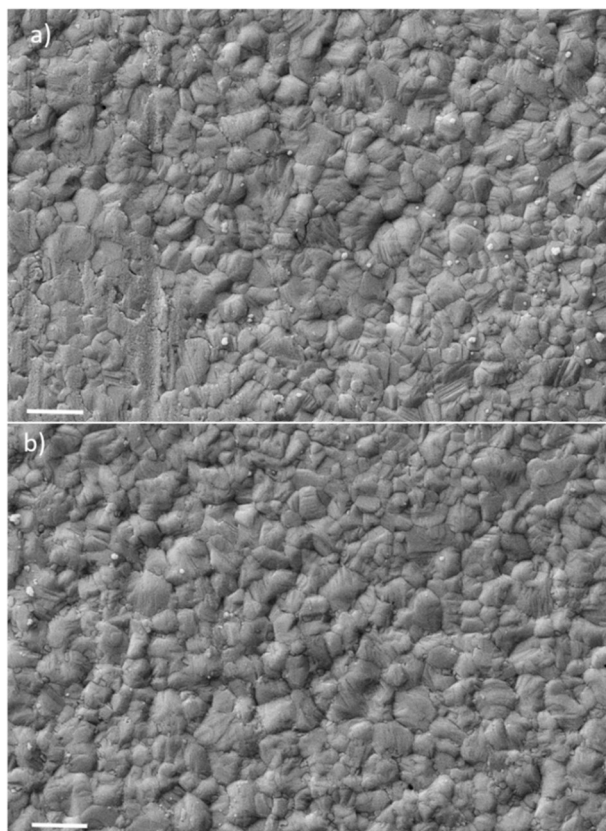


**Figure 1.** SEM image of the pristine (a) and TEOS-modified PS layers (b). The scale bar is 1 micron in both figures.

The absence of the delta phase could be originated by Cs ions, as explained before [13]. The FWHM of the main perovskite peak at  $14.10^\circ$  was obtained through fitting and was very similar, 0.19 and 0.20, respectively, for reference and TEOS-modified perovskite layers. The crystallite size of the perovskite layers was estimated by the Scherrer equation from the most intense peak at  $14.1^\circ$ , slightly reduced from 43 nm to 40.2 nm. Regarding the same position of perovskite diffraction peaks in reference and modified perovskite (PS) layers and a mere difference of FWHM, the provided results indicate that the structure of PS film remained unchanged after the mentioned modification. This could propose the same anti-solvent crystallization processes in reference and modified anti-solvents. Besides the FTO/TiO<sub>2</sub> diffraction patterns, cubic PbI<sub>2</sub> peaks were distinguished at both pristine and modified perovskite layers with a mere difference in intensity, which could be from the incomplete conversion of precursors to the black perovskite phase as the deposition is performed in the atmosphere environment here. It is known that PbI<sub>2</sub> could passivate the defects and enhance the device's performance. Nevertheless, excessive PbI<sub>2</sub> contents in the films adversely distress the device's performance by its poor optoelectronic properties [44]. It is known that after TEOS modification of the anti-solvent, a silica layer is

integrated with the perovskite layer through the hydrolysis reaction of the TEOS. However, no diffraction patterns of incorporated silica were identified, revealing that amorphous silica is formed on the perovskite layer through hydrolysis.

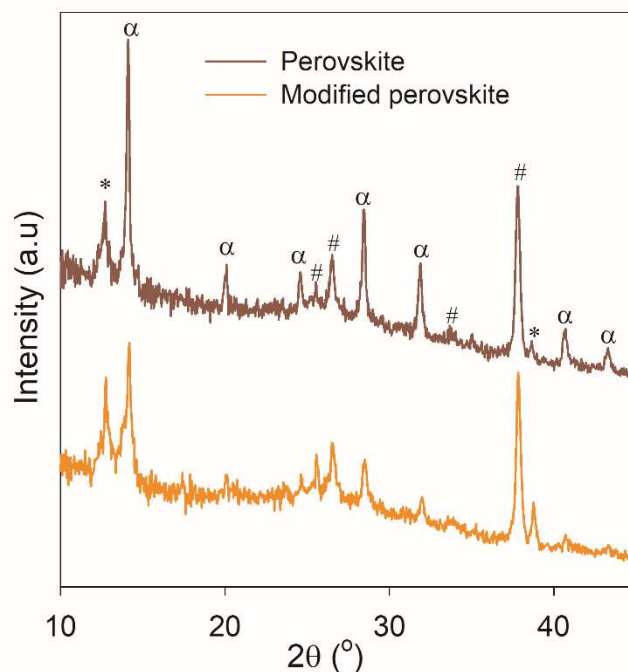


Figure 2. XRD spectra of pristine and modified perovskite films on FTO-coated glass/TiO<sub>2</sub> substrates. Perovskite, PbI<sub>2</sub>, and FTO/ TiO<sub>2</sub> diffraction peaks are indicated by  $\alpha$ , \*, and #, respectively.

Moreover, the ultraviolet–visible (UV–vis) absorption spectra of perovskite films were measured (not shown here), and a mere difference between pristine and modified PS film's absorption spectrum was observed. Furthermore, concerning

the Tauc plot method, the pristine and TEOS-modified PS band gaps had a comparable approximately 1.61 eV for both structures. These observations reveal that the TEOS modification has no marked effect on  $\text{Cs}_{0.05}(\text{MA}_{0.17}\text{FA}_{0.83})_{0.95}\text{Pb}(\text{I}_{0.83}\text{Br}_{0.17})_3$  PS layer regarding the optical properties. To explore the effect of TEOS-modified perovskite layers on the photovoltaic properties of PSCs, here reference and TEOS-modified cells were prepared. Figure 3 indicates the J-V curves of normal and modified cells. The photovoltaic parameters of cells are summarized in Table 1, concerning an apparent explanation. According to the results, a  $V_{oc}$  of 1 V, a  $J_{sc}$  of  $22.46 \text{ mA}\cdot\text{cm}^{-2}$ , a FF of 62.60 %, and a PCE of 14.06 % are obtained in normal cells. Notably, our cells are made under an ambient environment, and their efficiency is expected to be lower than the record efficiencies of triple-cation perovskite solar cells made under inert atmospheres like  $\text{N}_2$  or Ar [13]. The modified cell reveals a higher  $J_{sc}$  of  $23.39 \text{ mA}/\text{cm}^2$ ,  $V_{oc}$  of 1.03 V, and a considerably raised FF of 71.26 %, resulting in an improved efficiency of 17.16 %.

A glance at the graph and Table 1 reveals the superior photovoltaic properties of modified cells compared to pristine ones, primarily by soaring the fill factor (from 62.60 % in normal cells to 71.26 % in modified cells). At the same time, the  $V_{oc}$  and  $J_{sc}$  have a mere difference.

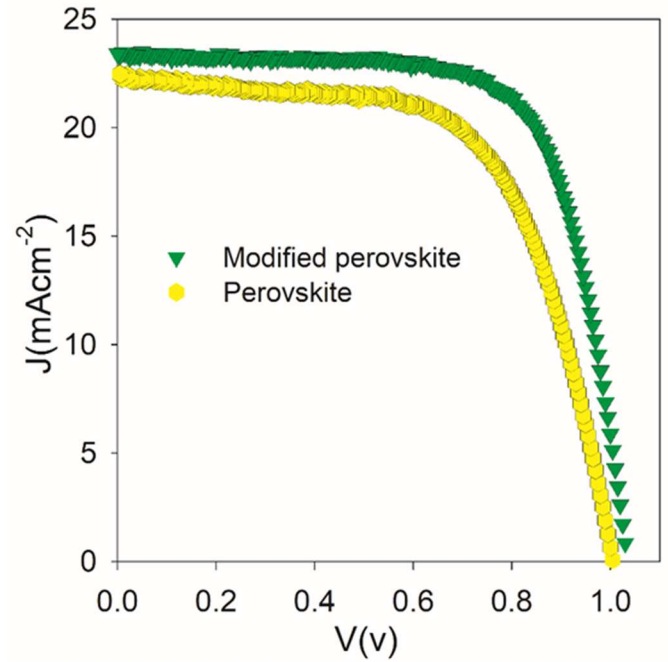


Figure 3. J-V curves of solar cells: made with normal or modified perovskite layers.

**Table 1.** Photovoltaic parameters of cells: photocurrent  $j_{sc}$ , open circuit voltage  $V_{oc}$ , fill factor FF, and efficiency PCE, for normal and modified cells.

Cell type	$V_{oc}$ (V)	$J_{sc}$ ( $\text{mA}/\text{cm}^2$ )	FF(%)	PCE (%)
Normal Cell	1.00	22.46	62.60	14.06±0.22
Modified Cell	1.03	23.39	71.26	17.16±0.13

Steady-state photoluminescence (PL) measurements were conducted on pristine and modified PS layers to evaluate the origin of improved photovoltaic properties of modified cells. **Error! Reference source not found.**4 reveals the PL spectra of the pristine and modified  $\text{Cs}_{0.05}(\text{MA}_{0.17}\text{FA}_{0.83})_{0.95}\text{Pb}(\text{I}_{0.83}\text{Br}_{0.17})_3$  PS films. The PL peak is located at 765 nm for both cells, while the PL intensity is markedly raised after modification. These results suggest a significant dropping in the density of trap states in the PS layers as non-radiative recombination centers. In contrast, the bulk properties of the layer are unchanged, according to figures 1-2.

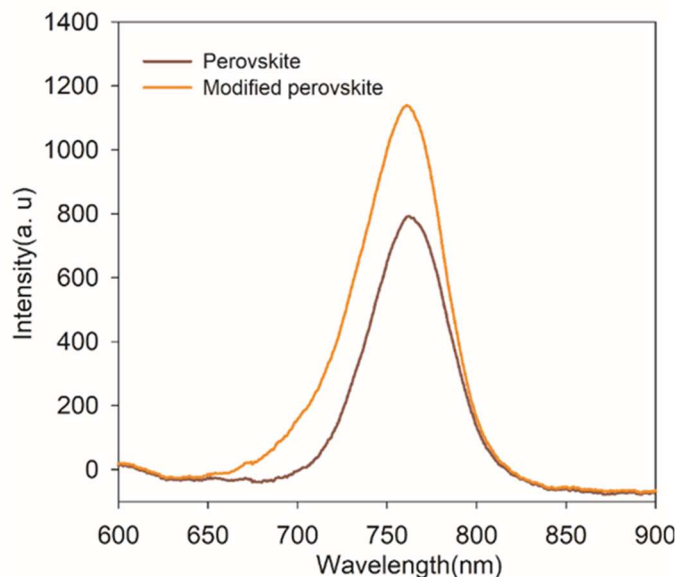


Figure 4. Comparison of photoluminescence emission spectra of normal  $\text{Cs}_{0.05}(\text{MA}_{0.17}\text{FA}_{0.83})_{0.95}\text{Pb}(\text{I}_{0.83}\text{Br}_{0.17})_3$  PS and TEOS modified PS films.

The density of trap states was measured through the SCLC experiment (Figure 5), which was carried out on the hole-only devices with ITO/ $\text{NiO}_x$ /Perovskite/CIS/Au structure (inset of Figure 5).

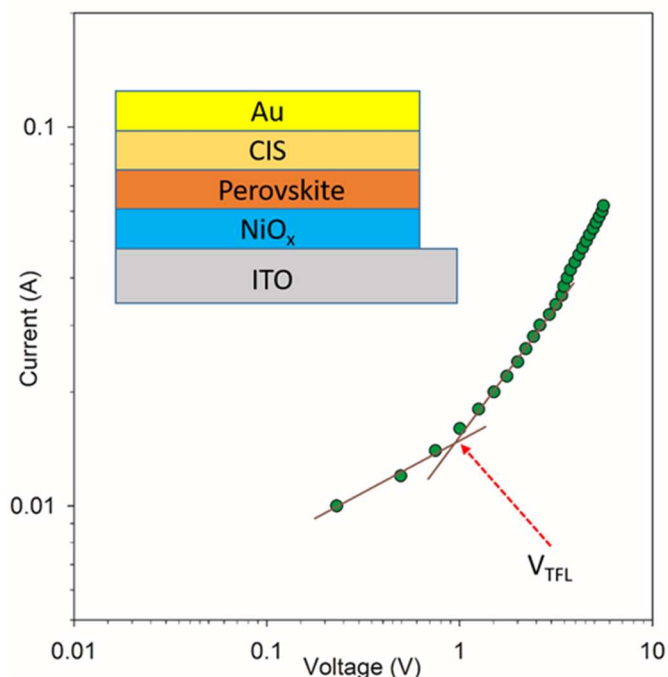


Figure 5. Typical current-voltage properties of the hole-only devices with ITO/ $\text{NiO}_x$ /Perovskite/CIS/Au structure as presented in the inset of the figure.

The density of the trap states was determined by the trap-filled-limit voltage ( $V_{\text{TFL}}$ ) in the equation  $V_{\text{TFL}} = 0.5 e D_{\text{trap}} L^2 \epsilon^{-1} \epsilon_0^{-1}$ , where  $e$ ,  $\epsilon_0$ ,  $\epsilon$ ,  $L$ , and  $D_{\text{trap}}$  are elementary charge, vacuum permittivity, relative dielectric constant (28.8 for PS layer), the thickness of the PS layer, and the density of trap states respectively [45, 46]. The

corresponding trap densities were obtained for normal and modified devices according to Table

2 (each measurement was conducted on at least three normal/modified cells).

Table 2: Trap densities of normal and modified devices (each measurement was conducted on at least three normal/modified cells).

Cell type	Sample number	$N_t$
Normal	1	$1.63 \times 10^{16} \text{Cm}^{-3}$
Normal	2	$1.69 \times 10^{16} \text{Cm}^{-3}$
Normal	3	$1.74 \times 10^{16} \text{Cm}^{-3}$
Modified	1	$1.41 \times 10^{16} \text{Cm}^{-3}$
Modified	2	$1.46 \times 10^{16} \text{Cm}^{-3}$
Modified	3	$1.49 \times 10^{16} \text{Cm}^{-3}$

The SCLC measurement data shows the positive effect of perovskite modification so that the trap density in the modified sample is reduced compared to the pristine perovskite. The reduced surface trap states, which originated from the integrated amorphous silica in PS layers [47], could explain the improved fill factors and, consequently, higher efficiencies in modified cells, as explained in Table 1.

The results obtained from repeating the SCLC analysis are very close to each other, and this shows the accuracy of our measurements using the all-inorganic hole-only device structure.

#### 4. Conclusions

Here a simple all-inorganic hole-only device was introduced for exploring the density of trap states in the perovskite layer. To investigate the

performance of the hole-only device, here we made several cells with various pristine and silica-modified perovskite layers. According to our results, the crystalline structure and the optical properties of the perovskite layer were preserved after modification, while the surface trap states were decreased markedly. A considerable improvement in fill factors was obtained, which originated from the lower charge recombination in modified cells. As a general conclusion, a simple hole-only device structure is introduced to monitor the perovskite layers' defect properties and make layers with superior properties for high-efficiency PSCs.

#### References:

- (1) Roy P, Sinha NK, Tiwari S, Khare A. A review on perovskite solar cells: Evolution of architecture,

fabrication techniques, commercialization issues, and status. *Solar Energy*. 2020;198:665-88.

(2) Grätzel M. The rise of highly efficient and stable perovskite solar cells. *Accounts of chemical research*. 2017;50(3):487-91.

(3) Yi C, Luo J, Meloni S, Boziki A, Ashari-Astani N, Grätzel C, Zakeeruddin SM, R othlisberger U, Grätzel M. Entropic stabilization of mixed A-cation ABX<sub>3</sub> metal halide perovskites for high-performance perovskite solar cells. *Energy & Environmental Science*. 2016;9(2):656-62.

(4) Becker M, Kl uner T, Wark M. Formation of hybrid ABX<sub>3</sub> perovskite compounds for solar cell application: first-principles calculations of effective ionic radii and determination of tolerance factors. *Dalton Transactions*. 2017;46(11):3500-9.

(5) Yin WJ, Yang JH, Kang J, Yan Y, Wei SH. Halide perovskite materials for solar cells: a theoretical review. *Journal of Materials Chemistry A*. 2015;3(17):8926-42.

(6) Niu G, Guo X, Wang L. Review of recent progress in chemical stability of perovskite solar cells. *Journal of Materials Chemistry A*. 2015;3(17):8970-80.

(7) Dubey A, Adhikari N, Mabrouk S, Wu F, Chen K, Yang S, Qiao Q. A strategic review on processing routes towards highly efficient perovskite solar cells. *Journal of Materials Chemistry A*. 2018;6(6):2406-31.

(8) Gapol MA, Balanay MP, Kim DH. Molecular engineering of tetraphenyl benzidine-based hole transport material for perovskite solar cell. *The Journal of Physical Chemistry A*. 2017;121(6):1371-80.

(9) Ye J, Zhang X, Zhu L, Zheng H, Liu G, Wang H, Hayat T, Pan X, Dai S. Enhanced morphology and stability of high-performance perovskite solar cells with ultra-smooth surface and high fill factor via crystal growth engineering. *Sustainable Energy & Fuels*. 2017;1(4):907-14.

(10) Conings B, Drijkoningen J, Gauquelin N, Babayigit A, D'Haen J, D'Olieslaeger L, Ethirajan A, Verbeeck J, Manca J, Mosconi E, Angelis FD. Intrinsic thermal instability of methylammonium lead trihalide perovskite. *Advanced Energy Materials*. 2015;5(15):1500477.

(11) Misra RK, Aharon S, Li B, Mogilyansky D, Visoly-Fisher I, Etgar L, Katz EA. Temperature-and component-dependent degradation of perovskite photovoltaic materials under concentrated sunlight. *The journal of physical chemistry letters*. 2015;6(3):326-30.

(12) Hoke ET, Slotcavage DJ, Dohner ER, Bowring AR, Karunadasa HI, McGehee MD. Reversible photo-induced trap formation in mixed-halide hybrid perovskites for photovoltaics. *Chemical Science*. 2015;6(1):613-7.

(13) Saliba M, Matsui T, Seo JY, Domanski K, Correa-Baena JP, Nazeeruddin MK, Zakeeruddin SM, Tress W, Abate A, Hagfeldt A, Grätzel M. Cesium-containing triple cation perovskite solar cells: improved stability, reproducibility and high efficiency. *Energy & environmental science*. 2016;9(6):1989-97.

(14) Eperon GE, Stranks SD, Menelaou C, Johnston MB, Herz LM, Snaith HJ. Formamidinium lead trihalide: a broadly tunable perovskite for efficient planar heterojunction solar cells. *Energy & Environmental Science*. 2014;7(3):982-8.

(15) Yi C, Luo J, Meloni S, Boziki A, Ashari-Astani N, Grätzel C, Zakeeruddin SM, R othlisberger U, Grätzel M. Entropic stabilization of mixed A-cation ABX<sub>3</sub> metal halide perovskites for high performance perovskite solar cells. *Energy & Environmental Science*. 2016;9(2):656-62.

(16) Parrott ES, Milot RL, Stergiopoulos T, Snaith HJ, Johnston MB, Herz LM. Effect of structural phase transition on charge-carrier lifetimes and defects in CH<sub>3</sub>NH<sub>3</sub>SnI<sub>3</sub> perovskite. *The journal of physical chemistry letters*. 2016;7(7):1321-6.

- (17) Slotcavage DJ, Karunadasa HI, McGehee MD. Light-induced phase segregation in halide-perovskite absorbers. *ACS Energy Letters*. 2016;1(6):1199-205.
- (18) Song D, Ji J, Li Y, Li G, Li M, Wang T, Wei D, Cui P, He Y, Mbengue JM. Degradation of organometallic perovskite solar cells induced by trap states. *Applied Physics Letters*. 2016;108(9):093901.
- (19) Xia R, Fei Z, Drigo N, Bobbink FD, Huang Z, Jasiūnas R, Franckevičius M, Gulbinas V, Mensi M, Fang X, Roldán-Carmona C. Retarding Thermal Degradation in Hybrid Perovskites by Ionic Liquid Additives. *Advanced Functional Materials*. 2019;29(22):1902021.
- (20) Nie W, Tsai H, Asadpour R, Blancon JC, Neukirch AJ, Gupta G, Crochet JJ, Chhowalla M, Tretiak S, Alam MA, Wang HL. High-efficiency solution-processed perovskite solar cells with millimeter-scale grains. *Science*. 2015;347(6221):522-5.
- (21) Qiu W, Merckx T, Jaysankar M, De La Huerta CM, Rakocevic L, Zhang W, Paetzold UW, Gehlhaar R, Froyen L, Poortmans J, Cheyns D. Pinhole-free perovskite films for efficient solar modules. *Energy & Environmental Science*. 2016;9(2):484-9.
- (22) Ishikawa R, Ueno K, Shirai H. Highly crystalline large-grained perovskite films using two additives without an antisolvent for high-efficiency solar cells. *Thin Solid Films*. 2019;679:27-34.
- (23) Sheibani E, Heydari M, Ahangar H, Mohammadi H, Fard HT, Taghavinia N, Samadpour M, Tajabadi F. 3D asymmetric carbazole hole transporting materials for perovskite solar cells. *Solar Energy*. 2019 ;189:404-11.
- (24) Ono LK, Juarez-Perez EJ, Qi Y. Progress on perovskite materials and solar cells with mixed cations and halide anions. *ACS applied materials & interfaces*. 2017 ;9(36):30197-246.
- (25) Zhao D, Ke W, Grice CR, Cimaroli AJ, Tan X, Yang M, Collins RW, Zhang H, Zhu K, Yan Y. Annealing-free efficient vacuum-deposited planar perovskite solar cells with evaporated fullerenes as electron-selective layers. *Nano Energy*. 2016;19:88-97.
- (26) Xiao Z, Dong Q, Bi C, Shao Y, Yuan Y, Huang J. Solvent annealing of perovskite-induced crystal growth for photovoltaic-device efficiency enhancement. *Advanced Materials*. 2014;26(37):6503-9.
- (27) Liu J, Gao C, He X, Ye Q, Ouyang L, Zhuang D, Liao C, Mei J, Lau W. Improved crystallization of perovskite films by optimized solvent annealing for high efficiency solar cell. *ACS applied materials & interfaces*. 2015;7(43):24008-15.
- (28) Burschka J, Pellet N, Moon SJ, Humphry-Baker R, Gao P, Nazeeruddin MK, Grätzel M. Sequential deposition as a route to high-performance perovskite-sensitized solar cells. *Nature*. 2013;499(7458):316-9.
- (29) Sanchez S, Christoph N, Grobety B, Phung N, Steiner U, Saliba M, Abate A. Efficient and stable inorganic perovskite solar cells manufactured by pulsed flash infrared annealing. *Advanced Energy Materials*. 2018 ;8(30):1802060
- (30) Jeon NJ, Noh JH, Kim YC, Yang WS, Ryu S, Seok SI. Solvent engineering for high-performance inorganic-organic hybrid perovskite solar cells. *Nature materials*. 2014 ;13(9):897-903.
- (31) Kim GW, Kang G, Choi K, Choi H, Park T. Solution Processable Inorganic–Organic Double-Layered Hole Transport Layer for Highly Stable Planar Perovskite Solar Cells. *Advanced Energy Materials*. 2018;8(26):1801386.
- (32) Lee J, Malekshahi Byranvand M, Kang G, Son SY, Song S, Kim GW, Park T. Green-solvent-processable, dopant-free hole-transporting materials for robust and

- efficient perovskite solar cells. *Journal of the American Chemical Society*. 2017;139(35):12175-81.
- (33) Perumallapelli GR, Vasa SR, Jang J. Improved morphology and enhanced stability via solvent engineering for planar heterojunction perovskite solar cells. *Organic Electronics*. 2016;31:142-8.
- (34) Zhao D, Yu Y, Wang C, Liao W, Shrestha N, Grice CR, Cimaroli AJ, Guan L, Ellingson RJ, Zhu K, Zhao X. Low-bandgap mixed tin-lead iodide perovskite absorbers with long carrier lifetimes for all-perovskite tandem solar cells. *Nature Energy*. 2017 ;2(4):17018.
- (35) Lin N, Qiao J, Dong H, Ma F, Wang L. Morphology-controlled CH<sub>3</sub>NH<sub>3</sub>PbI<sub>3</sub> films by hexane-assisted one-step solution deposition for hybrid perovskite mesoscopic solar cells with high reproductivity. *Journal of Materials Chemistry A*. 2015;3(45):22839-45.
- (36) Yin M, Xie F, Chen H, Yang X, Ye F, Bi E, Wu Y, Cai M, Han L. Annealing-free perovskite films by instant crystallization for efficient solar cells. *Journal of Materials Chemistry A*. 2016;4(22):8548-53.
- (37) Paek S, Schouwink P, Athanasopoulou EN, Cho KT, Grancini G, Lee Y, Zhang Y, Stellacci F, Nazeeruddin MK, Gao P. From nano-to micrometer scale: the role of antisolvent treatment on high performance perovskite solar cells. *Chemistry of Materials*. 2017;29(8):3490-8.
- (38) Prochowicz D, Tavakoli MM, Solanki A, Goh TW, Pandey K, Sum TC, Saliba M, Yadav P. Understanding the effect of chlorobenzene and isopropanol anti-solvent treatments on the recombination and interfacial charge accumulation in efficient planar perovskite solar cells. *Journal of Materials Chemistry A*. 2018;6(29):14307-14.
- (39) Jin S, Wei Y, Huang F, Yang X, Luo D, Fang Y, Zhao Y, Guo Q, Huang Y, Wu J. Enhancing the perovskite solar cell performance by the treatment with mixed anti-solvent. *Journal of Power Sources*. 2018;404:64-72.
- (40) Yu Y, Yang S, Lei L, Cao Q, Shao J, Zhang S, Liu Y. Ultrasoother perovskite film via mixed anti-solvent strategy with improved efficiency. *ACS applied materials & interfaces*. 2017;9(4):3667-76.
- (41) Khorasani, A.; Marandi, M.; Khosroshahi, R.; Malekshahi Byranvand, M.; Dehghani, M.; Iraj Zad, A.; Tajabadi, F.; Taghavinia, N. Optimization of CuIn<sub>1-x</sub>Ga<sub>x</sub>S<sub>2</sub> Nanoparticles and Their Application in the Hole-Transporting Layer of Highly Efficient and Stable Mixed-Halide Perovskite Solar Cells. 2019, *ACS applied materials & interfaces*, 11(34), 30838-30845.
- (42) Bi D, Yi C, Luo J, Décoppet JD, Zhang F, Zakeeruddin SM, Li X, Hagfeldt A, Grätzel M. Polymer-templated nucleation and crystal growth of perovskite films for solar cells with efficiency greater than 21%. *Nature Energy*. 2016;1(10):1-5.
- (43) Saki, Z.; Sveinbjörnsson, K.; Boschloo, G.; Taghavinia, N. The Effect of Lithium Doping in Solution-Processed Nickel Oxide Films for Perovskite Solar Cells. *ChemPhysChem*, 2019, 20(24), 3322-3327.
- (44) Chen Y, Meng Q, Xiao Y, Zhang X, Sun J, Han CB, Gao H, Zhang Y, Lu Y, Yan H. Mechanism of PbI<sub>2</sub> in Situ Passivated Perovskite Films for Enhancing the Performance of Perovskite Solar Cells. *ACS applied materials & interfaces*. 2019;11(47):44101-8.
- (45) Bube, R. H. Trap density determination by space-charge- limited currents. *J. Appl. Phys.* 1962, 33, 1733-1737.
- (46) Kumar, N.; Lee, H. B.; Hwang, S.; Kang, J. W. Large-area, green solvent spray deposited nickel oxide films for scalable fabrication of triple-cation perovskite solar cells. *J. Mater. Chem. A* 2020, 8, 3357-3368.



(47) Guan M, Zhang Q, Wang F, Liu H, Zhao J, Jia C, Chen Y. Employing tetraethyl orthosilicate additive to enhance trap passivation of planar perovskite solar cells. *Electrochimica Acta*. 2019;293:174-83.